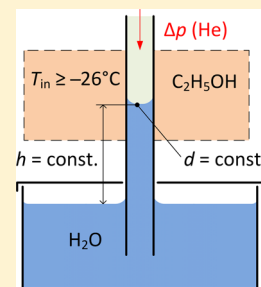


## Surface Tension of Supercooled Water Determined by Using a Counterpressure Capillary Rise Method

Václav Vinš,<sup>\*,†</sup> Maurice Fransen,<sup>†,‡</sup> Jiří Hykl,<sup>†</sup> and Jan Hrubý<sup>†</sup><sup>†</sup>Institute of Thermomechanics of the CAS, v. v. i., Dolejškova 5, Prague 8, 182 00, Czech Republic<sup>‡</sup>Eindhoven University of Technology, Den Dolech 2, 5612 AZ Eindhoven, The Netherlands

## Supporting Information

**ABSTRACT:** Measurements of the surface tension of supercooled water down to  $-25\text{ }^{\circ}\text{C}$  have been reported recently (Hrubý et al. *J. Phys. Chem. Lett.* **2014**, *5*, 425–428). These experiments did not show any anomalous temperature dependence of the surface tension of supercooled water reported by some earlier measurements and molecular simulations. In the present work, this finding is confirmed using a counterpressure capillary rise method (the *counterpressure method*) as well as through the use of the classical capillary rise method (the *height method*). In the *counterpressure method*, the liquid meniscus inside the vertical capillary tube was kept at a fixed position with an in-house developed helium distribution setup. A preset counterpressure was applied to the liquid meniscus when its temperature changed from a reference temperature ( $30\text{ }^{\circ}\text{C}$ ) to the temperature of interest. The magnitude of the counterpressure was adjusted such that the meniscus remained at the same height, thus compensating the change of the surface tension. One advantage of the *counterpressure method* over the *height method* consists of avoiding the uncertainty due to a possible variation of the capillary diameter along its length. A second advantage is that the equilibration time due to the capillary flow of the highly viscous supercooled water can be shortened. For both the *counterpressure method* and the *height method*, the actual results are relative values of surface tension with respect to the surface tension of water at the reference temperature. The combined relative standard uncertainty of the relative surface tensions is less than or equal to 0.18%. The new data between  $-26$  and  $+30\text{ }^{\circ}\text{C}$  lie close to the IAPWS correlation for the surface tension of ordinary water extrapolated below  $0.01\text{ }^{\circ}\text{C}$  and do not exhibit any anomalous features.



## INTRODUCTION

The surface tension of supercooled liquids, in particular, water and aqueous mixtures, is an important property both in academia and in industry. It plays an essential role in atmospheric research of the nucleation and growth of water droplets<sup>1</sup> and ice crystals.<sup>2</sup> It is known that water in clouds can persist in a supercooled liquid form at temperatures down to  $-38\text{ }^{\circ}\text{C}$ .<sup>3</sup> Manka et al.<sup>4</sup> recently showed that liquid water nanodroplets rather than ice crystals form by homogeneous nucleation at temperatures down to  $-73\text{ }^{\circ}\text{C}$ . Reliable data for the surface tension of supercooled aqueous systems are also important in technical applications such as operation of wind turbines,<sup>5</sup> aircraft icing,<sup>6</sup> or design of secondary refrigeration systems operating with brine.<sup>7</sup>

Compared to other fluids, water shows several anomalies at low temperatures, e.g., the well-known maximum in the liquid density at  $+4\text{ }^{\circ}\text{C}$  at atmospheric pressure. The unusual behavior of liquid water becomes more distinct in the metastable supercooled region below  $0\text{ }^{\circ}\text{C}$ . For instance, the isobaric heat capacity and the isothermal compressibility seemingly diverge (or approach a sharp maximum) when extrapolated to temperatures around  $-45\text{ }^{\circ}\text{C}$ , i.e., below the homogeneous nucleation temperature  $T_{\text{H}} = -38\text{ }^{\circ}\text{C}$  at atmospheric pressure.<sup>8</sup> On the basis of both the experimental and theoretical studies, Mishima and Stanley<sup>9</sup> proposed an explanation for some of these anomalies. The liquid–liquid phase transition (LLPT) hypothesis with the hypothesized second critical point of water

seems to provide a rational explanation of the anomalous thermophysical properties of supercooled water.<sup>10–12</sup>

Early measurements of the surface tension at subzero temperatures<sup>13,14</sup> indicated another anomaly of supercooled water: a distinct change in the temperature trend, called the second inflection point (SIP), in the surface tension of water.<sup>15,16</sup> Feeney and DeBenedetti<sup>17</sup> supported the existence of SIP with their model based on the van der Waals theory of interfaces combined with the LLPT hypothesis. Molecular simulations by Lü and Wei<sup>18</sup> also pointed to the existence of SIP at temperatures around  $+30\text{ }^{\circ}\text{C}$ . On the other hand, other molecular simulations, e.g., by Chen and Smith<sup>19</sup> or Viererblová and Kolafa,<sup>20</sup> did not indicate this anomaly. New measurements performed in this study down to  $-26\text{ }^{\circ}\text{C}$  show that the SIP anomaly expected in the temperature range from  $+30$  to  $-9\text{ }^{\circ}\text{C}$  seems to be an artifact in older experiments and molecular simulations.

Methods to measure the surface tension have been reviewed, e.g., by Fransen et al.<sup>21</sup> or Adamson and Gast.<sup>22</sup> The usual tensiometric techniques cannot be employed for measurements under metastable supercooled conditions, because they require relatively large volumes of the liquid. The probability of the appearance of an ice nucleus within the time scale of the

Received: January 19, 2015

Revised: March 4, 2015

experiment is proportional to the sample volume.<sup>23</sup> Moreover, small samples can be cooled more rapidly and the experimental time scale can be shortened. It is thus desirable that the sample volume under the metastable condition is as small as possible. Furthermore, contacts with solid surfaces promoting crystallization must be avoided and the liquid samples have to be chemically pure and free of mechanical particles to suppress heterogeneous ice nucleation. Consequently, the methods used successfully for the measurement of the surface tension of supercooled water employ short columns of liquid in glass or fused silica capillary tubes.<sup>14,16,24</sup>

In the early days of surface tension measurement, the purity of water samples and the quality of capillary tubes were troublesome criteria. Nonetheless, in 1895, Humphreys and Mohler<sup>13</sup> managed to measure the surface tension of pure water at subzero temperatures down to  $-8\text{ }^{\circ}\text{C}$  using the capillary rise technique. The first extensive data set for the surface tension of supercooled water was reported by Hacker<sup>14</sup> in 1951. Hacker's measurements were based on a method developed by Ferguson and Kennedy,<sup>25</sup> who used a horizontally oriented capillary tube, partially filled with liquid, with a gas counterpressure applied to one end of the capillary tube. A short water thread was loaded into the capillary tube such that one liquid meniscus was located at the planar open end of the capillary tube. The shape of the outer meniscus was at first concave but gradually became planar and, subsequently, changed into convex by applying an increasing counterpressure at the other end of the capillary tube.

The surface tension could be determined from the counterpressure corresponding to the plane meniscus by employing the Young–Laplace equation given as follows

$$\sigma = \frac{\Delta p d}{4 \cos \theta} \quad (1)$$

In eq 1,  $\Delta p$  denotes the pressure difference compared with the barometric pressure,  $d$  marks the inner diameter of the capillary tube, and  $\theta$  is the contact angle between water and the capillary wall, usually considered equal to zero for glass or fused silica. Hacker's data, measured down to  $-22.5\text{ }^{\circ}\text{C}$ , showed a clear inflection point at subzero temperatures (SIP) around  $-9\text{ }^{\circ}\text{C}$ .

Existence of SIP could not be confirmed nor denied by subsequent measurements made by Floriano and Angell<sup>24</sup> and Trinh and Ohsaka,<sup>26</sup> as both data sets showed relatively large scatter. Furthermore, the data by Trinh and Ohsaka<sup>26</sup> might have suffered from an experimental artifact, as it shows a significant offset from the IAPWS (International Association for the Properties of Water and Steam) standard for the surface tension of ordinary water<sup>27</sup> above the triple point. The IAPWS correlation approved for use at temperatures between the triple point and the critical point of water has the following form

$$\sigma_{\text{corr}}(T) = B\tau^{\mu}(1 + b\tau) \quad (2)$$

where  $\sigma_{\text{corr}}$  denotes the correlated surface tension,  $\tau = (T_c - T)/(T_c + 273.15)$  is the dimensionless distance from the critical temperature  $T_c = 373.946\text{ }^{\circ}\text{C}$ ,  $\mu = 1.256$  is a universal critical exponent, and the coefficients  $B$  and  $b$  have values  $235.8\text{ mN}\cdot\text{m}^{-1}$  and  $-0.625$ , respectively. Equation 2 is based on the correlation of Vargaftik et al.<sup>28</sup> updated by IAPWS for the ITS-90 temperature scale. It shows one inflection point at a temperature of  $256.46\text{ }^{\circ}\text{C}$ .

Recently, our group managed to make an important breakthrough in the discussion about SIP. Measurements by Hrubý et al.<sup>16</sup> did not confirm the existence of SIP or any other

anomaly in the temperature course of the surface tension of supercooled water down to  $-25\text{ }^{\circ}\text{C}$ . The data collected on two different apparatuses by two independent research groups from Prague and from Pilsen were in mutual agreement and could be relatively well reproduced by the IAPWS correlation (eq 2) extrapolated below  $0.01\text{ }^{\circ}\text{C}$ . Both experimental setups were based on the classical capillary rise technique modified for operation under the metastable supercooled conditions.

In this study, new data sets verifying our previous measurements<sup>16,29</sup> were collected. The Prague setup was modified such that it could be used for two slightly different measuring techniques: a classical capillary rise method (*height* technique) with improved accuracy and a new approach based on the counterpressure capillary rise method (*counterpressure* technique). The main goals of the present study were to improve the original measuring technique and to obtain a new consistent data set at a high degree of supercooling with smaller uncertainty. A more comprehensive description of the experimental setup and the evaluation of the surface tension is provided in comparison with the previous study.<sup>16</sup>

## EXPERIMENTAL METHODS

The *counterpressure* method, combining the classical capillary rise method with the counterpressure of inert gas, has been developed and used for measuring the surface tension of supercooled water. The liquid column elevated in a vertical capillary tube was kept at a constant height with the help of an in-house developed helium distribution setup. A counterpressure of helium was adjusted such that it compensated the change of the surface tension due to the temperature jump. Keeping the liquid meniscus at a fixed position within the capillary tube avoided the uncertainty from a possible variation of the capillary tube inner diameter along its length. Moreover, the equilibration time of the capillary flow of highly viscous supercooled water was reduced in the *counterpressure* method because of a constant height of the elevated liquid column. In addition to the *counterpressure* method, the classical capillary rise technique was employed for comparison. The *height* technique provided more accurate results compared to the previous study<sup>16</sup> thanks to a new device for the height measurement.

**Overview.** Figure 1 shows a schematic overview of the experimental apparatus. The measuring technique was based on a modification of the standard capillary rise approach.<sup>22,24</sup> A vertical capillary tube, whose lower end was submerged in a liquid container with a lid, was partly located in the laboratory

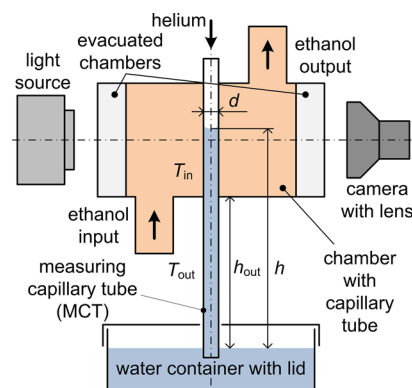
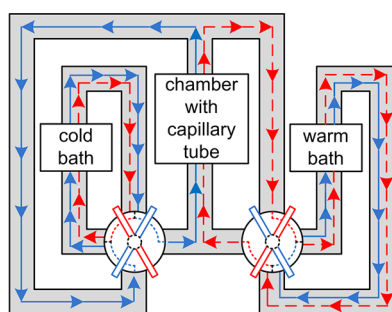


Figure 1. Scheme of the experimental apparatus.

environment and partly in a special in-house designed glass chamber. The lower part of the capillary tube together with the water container was kept at the ambient temperature  $T_{\text{out}}$ . The liquid container was positioned in such a way that the upper liquid meniscus inside the measuring capillary tube (MCT) was located approximately in the center of the glass chamber. The height of the outer part of the capillary tube slightly varied around  $h_{\text{out}} = 60$  mm. An external fan was blowing ambient air on the capillary tube to ensure a constant temperature  $T_{\text{out}}$  along the entire outer part. The upper part of the capillary tube, mounted in the glass chamber with inner temperature  $T_{\text{in}}$ , had a length of 45 mm. The liquid column inside the capillary tube elevated to a certain total height  $h$  resulting from the equilibrium between the surface forces and the pressure difference  $\Delta p$  in the Young–Laplace equation (eq 1).

The cylindrical glass chamber, insulated with 10 mm thick thermal foam insulation, was connected to two evacuated chambers on its bases through a set of optical windows. The evacuated chambers prevented condensation of air humidity on the optical windows at temperatures below the dew point temperature of ambient air. The temperature inside the glass chamber  $T_{\text{in}}$  was equal to the temperature of liquid ethanol flowing through the chamber. The ethanol was supplied by a temperature-control unit consisting of two separate thermostatic baths, two special in-house designed switch-valves allowing for fast switching between the two baths, and silicon tubing. The valves and the connecting tubing were insulated with thermal foam insulation. A scheme of the ethanol circuit is depicted in Figure 2. One bath was set to the desired measuring



**Figure 2.** Scheme of the ethanol circuit with switch-valves. The cold bath was set to the target temperature  $T$ , whereas the warm bath was kept at a constant reference temperature  $T_{\text{ref}}$ .

temperature  $T$ , while the other one was kept at a constant reference temperature  $T_{\text{ref}} = 30$  °C. Using two distinct thermostatic baths together with the switch-valves allowed rapid temperature transition and stabilization thanks to the high heat transfer of liquid ethanol. The temperature inside the chamber  $T_{\text{in}}$  stabilized within a maximum of 7 min after switching the valves. The subsequent measurement was carried out for 4–5 min. Fast temperature stabilization is a necessary condition to achieve a high supersaturation ratio, since the eventuality of the onset of nucleation of ice rapidly increases with time. Some other studies, e.g., Floriano and Angell,<sup>24</sup> employed cooling gases such as nitrogen with much lower heat transfer. An insufficient temperature stabilization with cooling gas could explain the rather large scatter of their data.<sup>24</sup>

The temperature was measured and logged at eight locations along the ethanol circuit. Most important was the temperature of the liquid ethanol inside the glass chamber in the region close to the capillary tube. It was measured by two Pt100

resistance thermometers connected to a digital thermometer bridge. The thermometers were calibrated against a secondary temperature standard. The standard uncertainty of the measured temperatures, including the effect of small temperature fluctuations, was better than 0.06 °C for all measurements.

The height of the liquid column inside the capillary tube was measured by a monochromatic high-resolution digital camera installed on a high-precision height gauge. The standard uncertainty of the total height was better than  $u(h) = 0.012$  mm. This represents a significant improvement compared to our previous measurements performed with a standard cathetometer with an uncertainty of 0.040 mm.<sup>16,29</sup>

The water-wetted material of all measuring capillary tubes was fused silica. Their inner diameter  $d$  was close to 0.32 mm; the accurate values and their uncertainties are discussed in the Results and Discussion section. The capillary tube was thoroughly cleaned with chromosulfuric acid and flushed with ultrapure water before each measurement series. After cleaning, the upper end of the capillary tube was immediately connected to a helium distribution setup to avoid any contact with ambient air. Application of pure helium reduced the risk of contamination of the inner surface by aerosol pollutants. Helium was chosen as the operating gas due to its low adsorption on the liquid surface and low solubility in water. From the measurements of Wiegand and Franck,<sup>30</sup> it follows that helium increases the surface tension by 0.002% at ambient temperature and pressure, which is 2 orders of magnitude below the expected uncertainty of the present results. The main atmospheric gases—nitrogen, oxygen, argon, and carbon dioxide—lower the surface tension of water by a few tenths of a percent compared to the surface tension of water in equilibrium with pure saturated vapor at ambient temperature and pressure.<sup>31,32</sup>

**Helium Distribution Setup.** The helium distribution setup was used (i) to ensure that the liquid meniscus is in contact with pure and particle-free helium, (ii) to flush the measuring capillary tube with helium to ensure that a fresh water sample is used for each measurement, and (iii) for the *counterpressure* method to maintain the meniscus at a constant height by a precisely adjusted counterpressure.

The helium distribution setup is sketched in Figure 3. Helium of declared purity 99.996% was further filtered by filter F1 to exclude particles down to 10 nm. The gas had to be clear of any organic vapors that could adsorb at the liquid meniscus and the fused silica surface and, consequently, affect the measured surface tension. Therefore, immediately before entering the measuring capillary tube (MCT), the gas passed through a hydrocarbon trap (F2) followed by a mechanical filter (F3) to capture particles possibly generated within the helium distribution setup (e.g., by operating the valves).

Helium was supplied from a gas bottle and depressurized to 0.5 MPa by a pressure regulator valve (PRV). From the PRV, helium flowed through an inlet capillary tube (ICT). The dimensions of this stainless steel capillary tube (inner diameter 0.25 mm, length 1.55 m) were chosen such that a standard flow rate of 200 cm<sup>3</sup> min<sup>-1</sup> was obtained. The major part of this flow was led to the bottom of a 1.0 m high water column (valve V1 being closed), thus generating a stable pressure reference of about 10 kPa. A metering needle valve enabled a fine adjustment of flow through the stainless steel outlet capillary tube (inner diameter 0.5 mm, length 70 mm). The maximum standard volume flow rate through this section was 13 cm<sup>3</sup> min<sup>-1</sup>



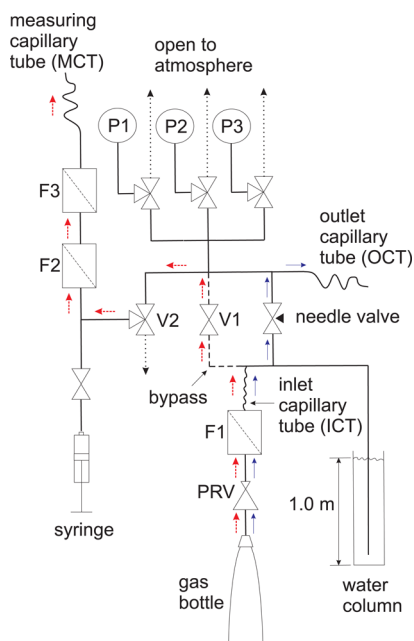


**Figure 3.** Scheme of the helium distribution setup. The flow direction in the *counterpressure* modus and in the helium flush is indicated by the solid blue arrows and the dashed red arrows, respectively.

when the needle valve was fully open. The pressure head generated at the outlet capillary tube was measured with three differential pressure transducers (P1, P2, and P3) with ranges of 150, 500, and 2500 Pa. Taking into account minute fluctuations of the helium overpressure by multiple readouts, the resulting standard uncertainty of overpressure measurement was determined as 0.36 Pa. The three-way valve V2 connected the measuring capillary tube to the helium overpressure when performing regular measurements with the *counterpressure* method. For comparative measurements at the reference temperature, and for the *height* method, valve V2 was vented to the atmosphere to enforce atmospheric pressure above the liquid meniscus. The vent of valve V2 was blown over by helium escaping from the outlet capillary tube (OCT) in order to prevent random inflow of air into the system. The vent was located at about the same elevation as the liquid meniscus (center of the glass chamber), so that the difference of densities of helium and air did not lead to a significant pressure head. In both measuring methods, the liquid content within the measuring capillary tube (MCT) was replaced before each measurement by fresh water from the liquid container. To this end, water was first repelled from the measuring capillary tube using a helium flush. An overpressure of 10 kPa was applied to the capillary tube by opening the bypass valve V1. After closing valve V1, the water column ascended toward the equilibrium height. In agreement with earlier studies,<sup>24</sup> we found that reproducible results were obtained with a descending meniscus. This observation can be explained by the roughness of the capillary tube surface and the need to form an adsorbed liquid layer smoothing the microscopically uneven surface. Formation of this layer in front of an ascending meniscus by a diffusion process is slow. A practical approach is to measure with a descending meniscus. In this case, the walls are wetted and the gas above the meniscus is fully saturated with water vapor. To measure with the descending meniscus, the liquid column was slightly lifted using a 2 mL syringe. The motion of the syringe created a pressure dip which then rapidly returned to the

adjusted overpressure, and the meniscus smoothly equilibrated at a well-reproducible position.

**Water.** Regular tap water was treated with a serially connected reverse osmosis unit and an analytical purification system. The resulting ultrapure water, with a constant resistivity of 18.2 MΩ·cm, free of particles larger than 0.2 μm, and total organic carbon content between 1 and 5 ppb, was used throughout all the measurements.

Further details about the components of the experimental apparatus are provided as Supporting Information.

## RESULTS AND DISCUSSION

In the present experimental study, the surface tension was determined from the Young–Laplace equation (eq 1). The total pressure difference from the barometric pressure  $\Delta p$  was given as a sum of the hydrostatic pressure of the elevated liquid column  $\Delta p_{\text{hyd}}$  and the helium overpressure above the liquid meniscus inside the measuring capillary tube (MCT)  $\Delta p_{\text{He}}$

$$\Delta p = \Delta p_{\text{hyd}} + \Delta p_{\text{He}} \quad (3)$$

The hydrostatic pressure was generated by the height of the liquid column. Because its temperature was nonuniform, we express it generally as

$$\Delta p_{\text{hyd}} = g \int_0^{h^*} \rho(z) dz \quad (4)$$

In eq 4,  $z$  denotes the vertical coordinate measured from the water container level and  $h^*$  marks the effective total height of the liquid column. The actually measured total height  $h$  spanned between the container level and the *bottom* of the meniscus. The effective total height includes the correction accounting for the weight of a meniscus with a nonzero contact angle

$$h^* = h + \frac{d}{6} \frac{1 - 3 \sin^2 \theta + 2 \sin^3 \theta}{\cos^3 \theta} \quad (5)$$

Equation 5 agrees with the direct numerical solution of the differential equation derived from the Young–Laplace equation<sup>22</sup> for circular capillary tubes with an inner diameter up to 3.0 mm. Consequently, other terms correcting for deviations of the meniscus shape from sphericity derived by Lord Rayleigh<sup>33</sup> are completely negligible for capillary tubes with  $d \approx 0.32$  mm.

The measuring apparatus was designed such that the temperature of the liquid column changed sharply from the ambient temperature  $T_{\text{out}}$  to the temperature inside the temperature-controlled chamber  $T_{\text{in}}$ . Therefore, it is practical to express the integral in eq 4 as

$$\Delta p_{\text{hyd}} = g [h^* \rho_{\text{in}} + h_{\text{out}} (\rho_{\text{out}} - \rho_{\text{in}}) + tq \rho_{\text{in}}] \quad (6)$$

where  $h_{\text{out}}$  is the height up to the middle of the temperature transition zone (see Figure 1),  $t$  is the height of the transition zone (not shown), and  $q$  is a dimensionless coefficient depending on the temperature profile in the transition zone and on the dependency of density on temperature between  $T_{\text{out}}$  and  $T_{\text{in}}$ . Coefficient  $q$  is defined in the following manner

$$q = \frac{1}{t \rho_{\text{in}}} \int_{h_{\text{out}} - t/2}^{h_{\text{out}} + t/2} \Delta \rho(z) dz \quad (7)$$

where  $\Delta \rho(z) = \rho(z) - \rho_{\text{out}}$  for  $z < h_{\text{out}}$  and  $\Delta \rho(z) = \rho(z) - \rho_{\text{in}}$  for  $z \geq h_{\text{out}}$ . We note that there is no approximation in the transformation of eq 4 into eq 6 with definition 7. Since the

height of the transition zone was quite small, it suffices to consider a linear temperature profile  $T(z)$  in the transition zone  $h_{\text{out}} - t/2 < z < h_{\text{out}} + t/2$ , allowing to express coefficient  $q$  exclusively based on the dependency  $\rho(T)$  as

$$q = \frac{1}{(T_{\text{in}} - T_{\text{out}})\rho_{\text{in}}} \int_{T_{\text{out}}}^{T_{\text{in}}} \Delta\rho(T) dT \quad (8)$$

where  $\Delta\rho(T) = \rho(T) - \rho_{\text{out}}$  if  $T - (T_{\text{out}} + T_{\text{in}})/2$  has the opposite sign as  $T - T_{\text{out}}$  and  $\Delta\rho(T) = \rho(T) - \rho_{\text{in}}$  otherwise.

Equation 6 is written in a form allowing one to appreciate the importance of the various heights and estimate their contribution to the uncertainty budget. Of the three heights  $h^*$ ,  $h_{\text{out}}$ , and  $t$ , the effective total height  $h^*$  is multiplied by a largest weight  $\rho_{\text{in}}$ . Because correction accounting for the meniscus weight (eq 5) is very small and accurate, the uncertainty of  $h^*$  is essentially equal to the uncertainty of the directly measured total height  $h$ , i.e.,  $u(h^*) \approx 0.012$  mm. The position of the temperature transition zone  $h_{\text{out}}$  was measured with an uncertainty of  $u(h_{\text{out}}) = 0.57$  mm; however, it is weighted by  $(\rho_{\text{out}} - \rho_{\text{in}})$ . The height of the transition zone was determined from the design of a screw cap on the chamber with the measuring capillary tube as  $t = 3.0 \pm 1.0$  mm. The uncertainty  $u(t)$  has a minor effect on the uncertainty budget, as the absolute value of coefficient  $q$  was always smaller than 0.008. The density of the stable and supercooled liquid water was evaluated from the IAPWS-95 equation of state<sup>34</sup> with uncertainties of 0.0001 and 0.03% above and below the triple point of water, respectively. The local gravity measured at our laboratory was taken as  $g = (98\,100\,7.0 \pm 1.0) \times 10^{-5} \text{ m}\cdot\text{s}^{-2}$ .

Figure 4 shows the helium overpressure  $\Delta p_{\text{He}}$  and the total pressure difference  $\Delta p$  for two independent data sets obtained

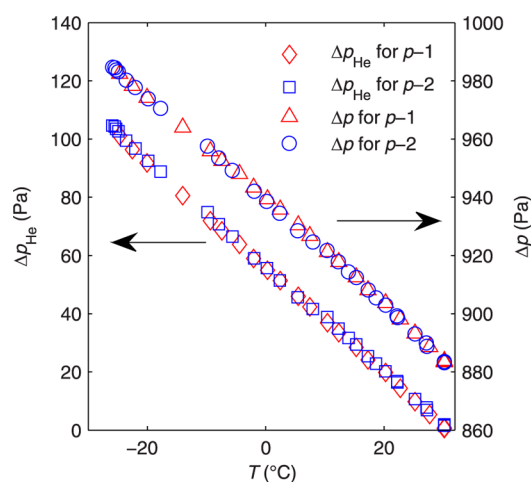


**Figure 4.** Helium overpressure  $\Delta p_{\text{He}}$  and total pressure difference  $\Delta p$  for the counterpressure measurements.

with the counterpressure method. Both pressures have an almost linear temperature trend. The hydrostatic pressure of the elevated water column,  $p_{\text{hyd}} = \Delta p - \Delta p_{\text{He}}$ , varied between 880 and 885 Pa with its highest value at 4 °C corresponding to the maximum in the liquid density of water.

A zero contact angle is usually considered for water and capillary tubes made of glass or fused silica.<sup>14,24</sup> In the present study, we took a more accurate value for a nonzero contact angle  $\theta = 3 \pm 1^\circ$  evaluated by Stepanov et al.<sup>35</sup> for the receding contact angle of water and fused silica. It is important to note that a constant temperature independent contact angle could be

considered in eq 1, as the present measurements were made at temperatures far below 200 °C where the receding contact angle starts to increase with temperature.<sup>36</sup>

The inner diameters of the employed capillary tubes  $d$  were first measured optically at the cuts of the capillary tubes. However, the uncertainty of these measurements would adversely affect the otherwise highly accurate measurements. For this reason, the inner diameters were determined by inverting eq 1 to fit the evaluated surface tension at a reference temperature of 30 and 20 °C for the counterpressure technique and the height technique, respectively, to the reference surface tension evaluated by the IAPWS correlation (eq 2). In this way, the present measurements are relative with respect to the value of surface tension at the reference temperature. The actual result of the present study is the relative surface tension  $Y$ , defined as

$$Y(T) = \frac{\sigma(T)}{\sigma_{\text{ref}}} \quad (9)$$

Using a different value for  $\sigma_{\text{ref}}$  for the evaluation of the experiment would not affect the evaluated relative surface tension; only the evaluated capillary tube diameters would be changed. The only place where the absolute value of the capillary tube diameter matters is correction of the meniscus weight (eq 5). This correction is very small, and taking any reasonable value for  $\sigma_{\text{ref}}$  will not result in an effect observable in the significant digits. We note that the relative surface tension is independent of gravity. In addition, some systematic errors, e.g., in the height or temperature measurement, cancel out to some extent. Ignoring these cancelations makes the present uncertainty estimates more conservative.

The inner diameter of the capillary tube  $d$  is an intermediate result which depends on the value of the reference surface tension. Consequently, it is appropriate to divide the relative total uncertainty  $u_r(d)$  into two independent contributions

$$u_r^2(d) = u_{r,\text{ref}}^2(d) + u_{r,Y}^2(d) \quad (10)$$

The first contribution is dominated by the relative uncertainty of the reference surface tension  $u_r(\sigma_{\text{ref}})$  and includes also the uncertainty of the relative uncertainty of the gravity  $u_r(g)$

$$u_{r,\text{ref}}^2(d) = u_r^2(\sigma_{\text{ref}}) + u_r^2(g) \quad (11)$$

The second contribution to the uncertainty of the capillary tube inner diameter  $u_{r,Y}(d)$  enters the uncertainty budget of the relative surface tension  $Y$ . This contribution includes the statistically evaluated uncertainty of repeated evaluations of the capillary tube diameter (A-type uncertainty) and uncertainties of the height gauge and temperature sensors based on their specifications and calibrations, and the uncertainty of the water density (B-type uncertainties).

The total relative uncertainty of the relative surface tension  $u_r(Y)$  includes the part of the capillary tube diameter  $u_{r,Y}(d)$  and further statistically evaluated scatter of the individual determinations of the relative surface tension and uncertainties of the measured height, temperature, and pressure (for the counterpressure method), and the uncertainty of the water density. The relative uncertainty of the evaluated relative surface tension was better than 0.18% for all measurements with both the height method and the counterpressure method.

While eq 9 provides the definition of the relative surface tension, the actual working expression is explicit in the absolute surface tension

$$\sigma(T) = Y(T)\sigma_{\text{ref}} \quad (12)$$

As explained before, the experimentally determined relative surface tension  $Y$  is independent of the reference surface tension  $\sigma_{\text{ref}}$ . Correspondingly, the uncertainty of the surface tension is obtained as

$$u_r^2(\sigma) = u_r^2(Y) + u_r^2(\sigma_{\text{ref}}) \quad (13)$$

For the absolute surface tensions provided in this work, the value of the reference surface tension was determined from the IAPWS correlation (eq 2), i.e.,  $\sigma_{\text{ref}} = \sigma_{\text{corr}}(T_{\text{ref}})$ . The IAPWS correlation<sup>27</sup> has relatively large uncertainty estimates at low temperatures close to the triple point, e.g.,  $u(\sigma_{\text{corr}}) = 0.36 \text{ mN}\cdot\text{m}^{-1}$  at 30 °C, thereby affecting the uncertainty of the surface tensions provided in this work. The uncertainty of the absolute surface tension evaluated using eq 13 lies between 0.36 and 0.41  $\text{mN}\cdot\text{m}^{-1}$  for temperatures between +30 and -26 °C, respectively, i.e., around 0.5%. When a more accurate value  $\sigma_{\text{ref}}$  becomes available for the surface tension at the reference temperature, the present relative measurements remain valid and the absolute surface tensions can be obtained by multiplying them with the new reference value. Correspondingly, the uncertainty of the absolute surface tensions will be modified according to eq 13. For example, Pallas and Harrison<sup>37</sup> at 20 and 25 °C declared much narrower uncertainties than the IAPWS standard.<sup>27</sup> However, a broad systematic study is needed to establish new generally accepted values for the surface tension of ordinary water at ambient temperatures and their uncertainties.

Tables 1 and 2 summarize the experimental data for the relative and absolute surface tension of the supercooled water. Each table includes two independent data sets. Results in Table 1 were obtained by the *counterpressure* method, while Table 2 contains data for the *height* technique. Both techniques resulted in a comparable relative standard uncertainty of the relative surface tension  $u_r(Y) \leq 0.18\%$ . The lower uncertainty for the data sets *h-2* and *p-2* was caused by different settings of the low-temperature thermostatic bath, improving the temperature stability inside the glass chamber. The measurement of each data point listed in Tables 1 and 2 was followed by a comparative measurement at the reference temperature that, consequently, avoided risk of accumulation of error possible by a continuous measurement. The inner diameters of the capillary tubes together with their uncertainties are provided in Table 3 for all four data sets. The relative uncertainty  $u_{r,\text{ref}}(d)$  from the uncertainties of the reference surface tension and the gravity is in all cases more than 3 times higher than the relative uncertainty  $u_{r,Y}(d)$  influencing the uncertainty of the relative surface tension  $Y$ .

Figure 5 shows the IAPWS correlation (eq 2) extrapolated to subzero temperatures compared with the new data obtained by both the *counterpressure* method and the *height* method. Literature data for the surface tension of supercooled water are also provided. The surface tension was measured down to -26 °C, which is 2 °C lower than in the previous study<sup>16</sup> (using the Prague setup). The higher supercooling and faster equilibration of temperature were mainly achieved by an improved design of the switch-valves with additional cooling channels. Nevertheless, the lowest temperature of -26 °C is still 12 °C above the homogeneous nucleation limit for pure water,  $T_{\text{H}} = -38$  °C.<sup>8</sup> Hence, there is probably some space left to achieve somewhat lower temperatures in the surface tension measurement.

**Table 1. Surface Tension of Supercooled Water Measured with the Counterpressure Technique**

$T$ (°C)	$Y$	$u(Y)$	$\sigma^a$ (mN/m)
Data Set <i>p-1</i> <sup>b</sup>			
-24.67	1.1111	0.0020	79.10
-22.54	1.1064	0.0019	78.76
-20.06	1.1018	0.0019	78.44
-14.01	1.0903	0.0019	77.62
-9.36	1.0811	0.0019	76.96
-7.39	1.0773	0.0019	76.69
-4.43	1.0723	0.0019	76.34
-2.05	1.0669	0.0019	75.95
0.31	1.0624	0.0019	75.63
5.49	1.0523	0.0019	74.91
10.42	1.0419	0.0019	74.17
15.30	1.0321	0.0018	73.48
20.26	1.0220	0.0018	72.76
25.23	1.0103	0.0018	71.92
30.21	0.9996	0.0018	71.16
Data Set <i>p-2</i> <sup>b</sup>			
-25.92	1.1141	0.0017	79.31
-25.53	1.1138	0.0017	79.29
-25.29	1.1129	0.0017	79.23
-24.89	1.1122	0.0017	79.18
-23.59	1.1091	0.0017	78.96
-21.99	1.1062	0.0017	78.75
-19.86	1.1018	0.0017	78.44
-17.75	1.0981	0.0017	78.17
-9.83	1.0833	0.0017	77.12
-7.92	1.0787	0.0017	76.79
-5.63	1.0740	0.0017	76.46
-1.94	1.0657	0.0016	75.87
0.21	1.0619	0.0016	75.60
5.41	1.0506	0.0016	74.79
10.39	1.0429	0.0016	74.24
15.29	1.0322	0.0016	73.48
20.24	1.0216	0.0016	72.73
25.22	1.0104	0.0016	71.93
30.19	0.9997	0.0015	71.17

$$^a\sigma = Y\sigma_{\text{ref}} \quad ^bT_{\text{ref}} = 30.00 \text{ °C}, \sigma_{\text{ref}} = 71.19 \text{ mN/m.}$$

As can be seen in Figure 6, which shows the deviation of the relative surface tension from the extrapolated IAPWS standard, the new data agree well with the previous capillary rise measurements. Moreover, the *counterpressure* data and the *height* data are in mutual agreement, proving the correctness of both measuring techniques. As a consequence, the assumption of a constant inner diameter of the capillary tubes employed in the *height* method was proven to be correct in our case. Variations of the inner diameter with height were not detected. The data indicate a systematically higher surface tension for supercooled water than the extrapolated IAPWS correlation (eq 2) at temperatures below -17 °C. The experimental surface tension is on average higher by 0.19  $\text{mN}\cdot\text{m}^{-1}$  than the extrapolated eq 2 at a temperature of -25 °C. The difference lies close to the uncertainty of the relative surface tension  $u(Y)$  and entirely within the uncertainty of the absolute surface tension  $u(\sigma)$  equal to 0.41  $\text{mN}\cdot\text{m}^{-1}$  at the lowest temperature.

Figure 7 shows the deviation of the *counterpressure* data and the literature data from the extrapolated IAPWS correlation (eq 2). A systematic deviation of Hacker's data<sup>14</sup> from both the new data and the extrapolated IAPWS correlation is clearly visible at

**Table 2. Surface Tension of Supercooled Water Measured with the Height Technique**

$T$ (°C)	$Y$	$u(Y)$	$\sigma^a$ (mN/m)
Data Set $h-1^b$			
-19.89	1.0779	0.0015	78.41
-13.94	1.0664	0.0015	77.57
-9.38	1.0583	0.0015	76.98
-6.85	1.0533	0.0015	76.62
-4.42	1.0493	0.0015	76.33
-1.94	1.0429	0.0014	75.86
0.28	1.0397	0.0014	75.63
2.67	1.0350	0.0014	75.29
5.49	1.0290	0.0014	74.85
10.34	1.0193	0.0014	74.14
15.29	1.0096	0.0014	73.44
20.24	0.9998	0.0014	72.73
25.22	0.9887	0.0014	71.92
30.20	0.9784	0.0014	71.17
Data Set $h-2^b$			
-25.18	1.0873	0.0015	79.09
-24.12	1.0853	0.0015	78.94
-22.54	1.0825	0.0014	78.74
-19.35	1.0768	0.0014	78.33
-2.95	1.0456	0.0014	76.06
-0.13	1.0402	0.0014	75.66
2.07	1.0357	0.0014	75.34
3.71	1.0329	0.0014	75.13
8.33	1.0235	0.0014	74.45
12.32	1.0158	0.0014	73.89
15.29	1.0096	0.0013	73.44
18.26	1.0033	0.0013	72.98
21.24	0.9969	0.0013	72.51
24.22	0.9909	0.0013	72.08
27.24	0.9846	0.0013	71.62
30.19	0.9783	0.0013	71.16

$$^a \sigma = Y \sigma_{\text{ref}} \quad ^b T_{\text{ref}} = 20.00 \text{ } ^\circ\text{C}, \quad \sigma_{\text{ref}} = 72.74 \text{ mN/m.}$$

**Table 3. Inner Diameter of the Capillary Tubes and Contributions to Its Relative Uncertainty Defined in eq 10**

data set	$d$ (mm)	$u_{r,\text{ref}}(d)$ (%)	$u_{r,Y}(d)$ (%)
$p-1$	0.3216	0.50	0.10
$p-2$	0.3217	0.50	0.10
$h-1$	0.3215	0.50	0.09
$h-2$	0.3218	0.50	0.09

temperatures below  $-9$  °C. The new data have relatively low scatter and good internal consistency compared to other data sets, e.g., by Floriano and Angell<sup>24</sup> or Trinh and Ohsaka.<sup>26</sup> The temperature trend of the measured surface tension supports the previous study<sup>16</sup> refuting the existence of SIP, expected in the temperature range from  $-9$  to  $+30$  °C, or any other anomaly in the surface tension of supercooled water. On the other hand, a small systematic offset of the new data from the extrapolated correlation (eq 2) is observed at temperatures below  $-17$  °C. This effect can be hardly qualified as indication of an anomaly. The measured data in the supercooled region lie close to a linear extrapolation of the IAPWS standard<sup>27</sup> from  $0.01$  °C (blue solid line in Figure 7). The present results of course do not exclude anomalous interfacial phenomena close to the homogeneous nucleation limit, or even at lower temperatures

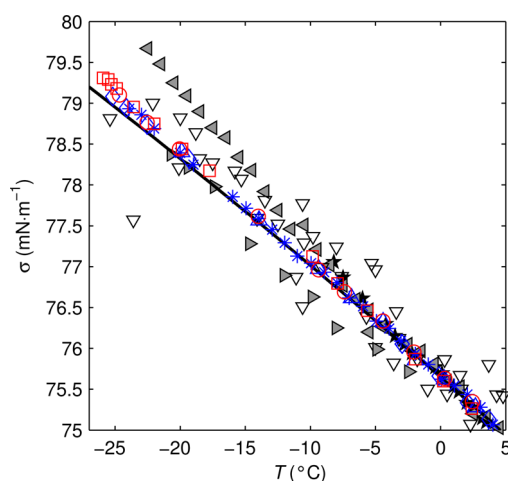


**Figure 5.** Comparison of the height and counterpressure data with the literature data. black —, IAPWS correlation (eq 2) extrapolated to temperatures below  $0.01$  °C; blue \*, previous height measurements<sup>16</sup> (Prague setup); red O, counterpressure data set  $p-1$ ; red □, counterpressure data set  $p-2$ ; blue ◇, height data set  $h-1$ ; blue △, height data set  $h-2$ ; ★, Humphreys and Mohler;<sup>13</sup> gray ◀, Hacker;<sup>14</sup> ▽, Floriano and Angell;<sup>24</sup> gray ▶, Trinh and Ohsaka.<sup>26</sup>

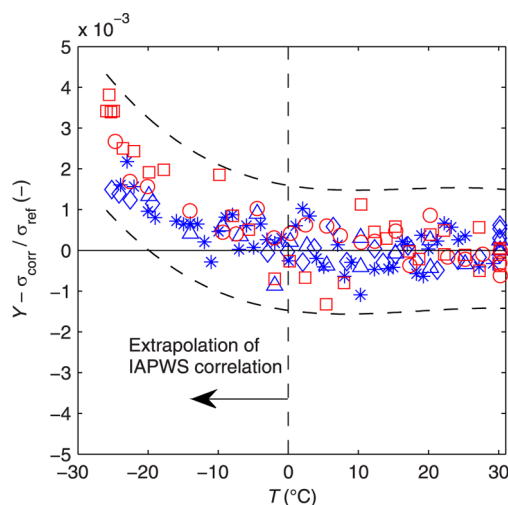


**Figure 6.** Deviation of the relative surface tension  $Y$  for the counterpressure method and the height technique from the IAPWS correlation (eq 2); blue \*, previous height measurements<sup>16</sup> (Prague setup); red O, counterpressure data set  $p-1$ ; red □, counterpressure data set  $p-2$ ; blue ◇, height data set  $h-1$ ; blue △, height data set  $h-2$ ; —, uncertainty range.

for microscopic droplets occurring in vapor-to-liquid nucleation studies.<sup>4,38,39</sup>

The new data are intended to be used in an update<sup>40</sup> of the existing IAPWS standard for the surface tension of ordinary water.<sup>27</sup> In particular, the range of validity of correlation 2 will be extended to the metastable supercooled region, which is of high importance, e.g., in atmospheric modeling. The accuracy of the current standard, especially its estimate of uncertainty at temperatures close to ambient, will also be improved. A better estimate of the uncertainty for the reference surface tension  $u(\sigma_{\text{ref}})$  can subsequently be used to improve the uncertainty of the absolute surface tension  $u(\sigma)$  determined in this study.



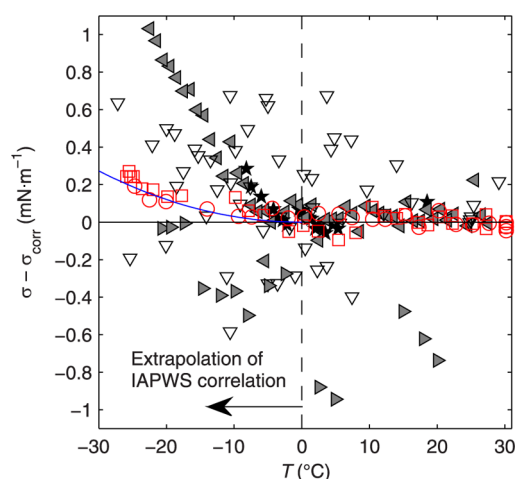


**Figure 7.** Deviation of the counterpressure data and the literature data for the surface tension  $\sigma$  from the IAPWS correlation (eq 2). red  $\circ$ , counterpressure data set  $p-1$ ; red  $\square$ , counterpressure data set  $p-2$ ;  $\star$ , Humphreys and Mohler;<sup>13</sup> gray  $\blacktriangleleft$ , Hacker;<sup>14</sup>  $\nabla$ , Floriano and Angell;<sup>24</sup> gray  $\blacktriangleright$ , Trinh and Ohsaka;<sup>26</sup> —, linear extrapolation of the IAPWS standard<sup>27</sup> from 0.01 °C.

## CONCLUSIONS

New experimental data for the surface tension of metastable supercooled water were measured in this study. A capillary rise technique designed for measurement with supercooled liquids was modified such that the liquid meniscus could be kept at a fixed position within a vertical capillary tube by applying a preset counterpressure of helium. Keeping the meniscus at constant height avoided the negative effect of a possible varying inner diameter along the capillary tube length and reduced the equilibration time due to the flow of the highly viscous supercooled water. In addition, the surface tension of supercooled water was measured with the classical capillary rise method, with improved accuracy compared to previous measurements.<sup>16,29</sup> The data obtained with the counterpressure technique and with the height method are in mutual agreement and support our previous measurements.<sup>16</sup> No anomaly in the surface tension of water was detected in the temperature range between  $-26$  and  $+30$  °C. A small systematic offset of the experimental data from the 1994 IAPWS correlation<sup>27</sup> for the surface tension of water extrapolated to subzero temperatures was detected at temperatures below  $-17$  °C. This deviation lies entirely within the uncertainty range for the absolute surface tension. However, it can point to a slightly incorrect behavior of the IAPWS correlation extrapolated to such low temperatures. Consequently, the presented data sets are important from the perspective of the planned extension of the IAPWS standard for the surface tension of ordinary water to the metastable supercooled region.

## ASSOCIATED CONTENT

### Supporting Information

A further description of the main components of the experimental setup. This material is available free of charge via the Internet at <http://pubs.acs.org>.

## AUTHOR INFORMATION

### Corresponding Author

\*Phone: +420 266 053 024. Fax: +420 286 584 695. E-mail: [vins@it.cas.cz](mailto:vins@it.cas.cz).

## Notes

The authors declare no competing financial interest.

## ACKNOWLEDGMENTS

The study was supported by Czech Science Foundation grant GJ15-07129Y, Ministry of Education CR grant LG13056, and institutional support RVO:61388998. The authors also thank Prof. M. E. H. van Dongen and Dr. E. W. Lemmon for carefully reading the manuscript and B. Šmíd and posthumously Dr. J. Blaha for their technical support.

## REFERENCES

- (1) Fransen, M. A. L. J.; Sachteleben, E.; Hrubý, J.; Smeulders, D. M. J. On the Growth of Homogeneously Nucleated Water Droplets in Nitrogen: An Experimental Study. *Exp. Fluids* **2014**, *55*, 1780-1–1780-17.
- (2) Earle, M. E.; Kuhn, T.; Khalizov, A. F.; Sloan, J. J. Volume Nucleation Rates for Homogeneous Freezing in Supercooled Water Microdroplets: Results from a Combined Experimental and Modelling Approach. *Atmos. Chem. Phys.* **2010**, *10*, 7945–7961.
- (3) Pruppacher, H. R.; Klett, J. D. *Microphysics of Clouds and Precipitation*, 1st ed.; Kluwer Group: Dordrecht, The Netherlands, 1978.
- (4) Manka, A.; Pathak, H.; Tanimura, S.; Wölk, J.; Strey, R.; Wyslouzil, B. E. Freezing Water in No-Man's Land. *Phys. Chem. Chem. Phys.* **2012**, *14*, 4505–4516.
- (5) Petit, J.; Bonaccorso, E. General Frost Growth Mechanism on Solid Substrates with Different Stiffness. *Langmuir* **2014**, *30*, 1160–1168.
- (6) Fernández-González, S.; Sánchez, J. L.; Gascón, E.; López, L.; García-Ortega, E.; Merino, A. Weather Features Associated with Aircraft Icing Conditions: A Case Study. *Sci. World J.* **2014**, 279063-1–279063-18.
- (7) Wang, K.; Eisele, M.; Hwang, Y.; Radermacher, R. Review of Second Loop Refrigeration Systems. *Int. J. Refrig.* **2010**, *33*, 212–234.
- (8) Kanno, H.; Speedy, R. J.; Angell, C. A. Supercooling of Water to  $-92$  °C under Pressure. *Science* **1975**, *189*, 880–881.
- (9) Mishima, O.; Stanley, H. E. The Relationship between Liquid, Supercooled and Glassy Water. *Nature* **1998**, *396*, 329–335.
- (10) Mishima, O. Volume of Supercooled Water under Pressure and the Liquid-Liquid Critical Point. *J. Chem. Phys.* **2010**, *133*, 144503-1–144503-6.
- (11) Holten, V.; Bertrand, C. E.; Anisimov, M. A.; Sengers, J. V. Thermodynamics of Supercooled Water. *J. Chem. Phys.* **2012**, *136*, 094507-1–094507-18.
- (12) Holten, V.; Anisimov, A. Entropy Driven Liquid-Liquid Separation in Supercooled Water. *Sci. Rep.* **2012**, *2*, 713-1–713-7.
- (13) Humphreys, W. J.; Mohler, J. F. Surface Tension of Water at Temperatures below Zero Degree Centigrade. *Phys. Rev.* **1895**, *2*, 387–391.
- (14) Hacker, P. T. *Experimental Values of the Surface Tension of Supercooled Water*, NACA TN 2510; **1951**.
- (15) Hrubý, J.; Holten, V. A Two-Structure Model of Thermodynamic Properties and Surface Tension of Supercooled Water. *Proceedings of the 14th International Conference on the Properties of Water and Steam*, **2005**; <http://www.iapws.jp/proceedings.html>.
- (16) Hrubý, J.; Vinš, V.; Mareš, R.; Hykl, J.; Kalová, J. Surface Tension of Supercooled Water: No Inflection Point down to  $-25$  °C. *J. Phys. Chem. Lett.* **2014**, *5*, 425–428.
- (17) Feeney, M. R.; Debenedetti, P. G. A Theoretical Study of the Interfacial Properties of Supercooled Water. *Ind. Eng. Chem. Res.* **2003**, *42*, 6396–6405.
- (18) Lü, Y. J.; Wei, B. Second Inflection Point of Water Surface Tension. *Appl. Phys. Lett.* **2006**, *89*, 164106-1–164106-3.
- (19) Chen, F.; Smith, P. E. Simulated Surface Tensions of Common Water Models. *J. Chem. Phys.* **2007**, *126*, 221101-1–221101-3.



- (20) Viererblová, L.; Kolafa, J. A Classical Polarizable Model for Simulations of Water and Ice. *Phys. Chem. Chem. Phys.* **2011**, *13*, 19925–19935.
- (21) Franses, E. I.; Basaran, O. A.; Chang, C. H. Techniques to Measure Dynamic Surface Tension. *Curr. Opin. Colloid Interface Sci.* **1996**, *1*, 296–303.
- (22) Adamson, A. W.; Gast, A. P. *Physical Chemistry of Surfaces*, 6th ed.; John Wiley & Sons: New York, 1997.
- (23) Sear, R. P. Estimation of the Scaling of the Nucleation Time with Volume when the Nucleation Rate Does Not Exist. *Cryst. Growth Des.* **2013**, *13*, 1329–1333.
- (24) Floriano, M. A.; Angell, C. A. Surface Tension and Molar Surface Free Energy and Entropy of Water to  $-27.2^{\circ}\text{C}$ . *J. Phys. Chem.* **1990**, *94*, 4199–4202.
- (25) Ferguson, A.; Kennedy, S. J. Notes on Surface-Tension Measurement. *Proc. Phys. Soc.* **1932**, *44*, 511–520.
- (26) Trinh, E.; Ohsaka, K. Measurement of Density, Sound Velocity, Surface Tension, and Viscosity of Freely Suspended Supercooled Liquids. *Int. J. Thermophys.* **1995**, *16*, 545–555.
- (27) IAPWS Release on Surface Tension of Ordinary Water Substance, 1994; <http://www.iapws.org/>.
- (28) Vargaftik, N. B.; Volkov, B. N.; Voljak, L. D. International Tables of the Surface Tension of Water. *J. Phys. Chem. Ref. Data* **1983**, *12*, 817–820.
- (29) Vinš, V.; Hrubý, J.; Hykl, J.; Blaha, J.; Šmíd, B. Design of an Experimental Apparatus for Measurement of the Surface Tension of Metastable Fluids. *EPJ Web Conf.* **2013**, *45*, 01094-1–01094-5.
- (30) Wiegand, G.; Franck, E. U. Interfacial Tension between Water and Non-Polar Fluids up to 473 K and 2800 bar. *Ber. Bunsen-Ges.* **1994**, *98*, 809–817.
- (31) Massoudi, R.; King, J. A. D. Effect of Pressure on the Surface Tension of Water: Adsorption of Low Molecular Weight Gases on Water at  $25^{\circ}$ . *J. Phys. Chem.* **1974**, *78*, 2262–2266.
- (32) Jho, C.; Nealon, D.; Shogbola, S.; King, A. D. Effect of Pressure on the Surface Tension of Water: Adsorption of Hydrocarbon Gases and Carbon Dioxide on Water at Temperatures between 0 and  $50^{\circ}\text{C}$ . *J. Colloid Interface Sci.* **1978**, *65*, 141–154.
- (33) Lord Rayleigh. On the Theory of the Capillary Tube. *Proc. R. Soc. A* **1916**, *92*, 184–195.
- (34) Wagner, W.; Pruss, A. The IAPWS Formulation 1995 for the Thermodynamic Properties of Ordinary Water Substance for General and Scientific Use. *J. Phys. Chem. Ref. Data* **2002**, *31*, 387–535.
- (35) Stepanov, V. G.; Volyak, L. D.; Tarlakov, Y. V. Wetting Contact Angles of Certain Systems. *J. Eng. Phys. Thermophys.* **1977**, *32*, 646–648. Translated from *Inzhenerno-Fizicheskii Zhurnal* **1977**, *32*, 1000–1003.
- (36) Volyak, L. D.; Stepanov, V. G.; Tarlakov, Y. V. Experimental Investigation of the Temperature Dependence of Wetting Angle of Water ( $\text{H}_2\text{O}$  and  $\text{D}_2\text{O}$ ) on Quartz and Sapphire. *Zh. Fiz. Khim.* **1975**, *49*, 2931–2933.
- (37) Pallas, N. R.; Harrison, Y. An Automated Drop Shape Apparatus and the Surface Tension of Pure Water. *Colloids Surf.* **1990**, *43*, 169–194.
- (38) Wölk, J.; Strey, R. Homogeneous Nucleation of  $\text{H}_2\text{O}$  and  $\text{D}_2\text{O}$  in Comparison: The Isotope Effect. *J. Phys. Chem. B* **2001**, *105*, 11683–11701.
- (39) Holten, V.; Labetski, D. G.; van Dongen, M. E. H. Homogeneous Nucleation of Water Between 200 and 240 K: New Wave Tube Data and Estimation of the Tolman Length. *J. Chem. Phys.* **2005**, *123*, 104505-1–104505-9.
- (40) Minutes from 2014 IAPWS Meeting, TPWS/SCSW Working Group, 2014, Moscow; <http://www.iapws.org/>.